The functional roles of time delay on flexible phase-locking in Bipedal locomotion

Weng, Wulin

Ei, Shin-Ichiro

Ohgane, Kunishige

出版情報：Journal of Math-for-Industry (JMI). 4 (B), pp.123-133, 2012-10. Faculty of Mathematics, Kyushu University
バージョン：
権利関係：

Journal of Math-for-Industry, Vol. 4 (2012B-7), pp. 123–133

Math-for-industry
Education & Research Hub

The functional roles of time delay on flexible phase-locking in Bipedal locomotion

Wulin Weng, Shin-Ichiro Ei and Kunishige Ohgane

Received on August 25, 2012 / Revised on September 14, 2012

Abstract. Based on neurophysiological studies, a walking model has been proposed, which is the coupling of two oscillatory systems, i.e., a central pattern generator (CPG) and a musculoskeletal system (Body). The walking model can well reproduce human walking. However, time delays on a sensorimotor loop give a serious problem in motor control in general. Indeed even a short time delay induces the walking model to fall. Theoretical studies have shown that the walking model can overcome the time delays by the flexible-phase locking. It emerges from the following two conditions; 1) activity of CPG and Body has stability of limit cycle; 2) a sign differs between coupling coefficients of the connection from Body to CPG and from CPG to Body, i.e., the afferent and efferent connection. Physical or physiological interpretation of this two theoretical conditions is an important problem. The condition 1) has already interpreted [1]. In this paper, we gain a physical interpretation of the condition 2). We introduce the simplified model fit to best analyze. Analyzing the simplified model, this study leads to the interpretation in which signs of the coupling coefficients corresponding to the excitatory and inhibitory connection are regarded as a force to forward and backward shift the CPG activity, respectively. This is an essential element to yield the flexible-phase locking.

Keywords. human walking, CPG, body, time delay, phase shift

1. Introduction

Neurophysiological studies [2, 3, 4, 5] have shown that signal transmission involves long time delay (more than 100ms) on sensorimotor loops in human locomotion system. In general, the time delay gives a serious problem for motor control in control engineering, in which it is dealt with as dead time. Based on neurophysiological evidence [6, 7, 8], Taga et al. [9] have modeled the human walking system, which is the coupled system of two oscillatory systems, i.e., a central pattern generator (CPG) and a musculoskeletal system (Body). Indeed, their walking model has shown to be fallen even by a short time delay (70ms) on the loop between CPG and Body. By using the model simplified the coupled system of CPG and Body, theoretical studies [1] have shown that both of the walking model and the simplified model can overcome loop time delay by its own function latent in the coupled two dynamics, i.e., the 'flexible-phase locking'. The flexible-phase locking is the function which induces the CPG phase to forward shift adaptively to time delay. Indispensability of neuronal activity's phase shift according to time delay for walking systems and the reason why Taga's walking model [9] cannot yield such phase shift are mentioned in detail in the studies [1]. The flexible-phase locking emerges from the following two conditions; 1) activity of CPG and Body has stability of limit cycle; 2) a sign differs between coupling coefficients of the connection from Body to CPG and from CPG to Body, i.e., the afferent and efferent connection. Physical or physiological interpretation of this two theoretical conditions is an important problem. The condition 1) is easy to interpret because of the property of their activities already shown in the studies [1]. On the other hand, understanding of the condition 2) has been an open question. The expression of the two conditions is confined to only mathematical understanding, although the conditions have been looked for as mechanisms of physical or physiological phenomena. Thus, this problem is important for scientific fields such as neurophysiology, physics, and mathematical science. This study is directed toward physical or physiological understanding of the condition 2), i.e., a sign difference between afferent and efferent coupling coefficients, which is required for establishing the flexible-phase locking.

From a viewpoint of the solution orbit, the walking model [1] can be characterized by the following two; a) CPG has an asymptotically stable limit cycle and Body oscillation could also be characterized by a limit cycle. b) the phase of the neuron output (CPG activity) shifted quarter period ahead of the joint motion (Body activity) without the time delay and the phase shift increases in proportion to time delay interval.

The simplified model [1] could reproduce the two characteristics a) and b). However, in the simplified model, limit cycles have been constructed by the perturbation of har-

monic oscillators in the Van der Pol equation. Therefore, it is difficult to quantitatively analyze the mechanisms of flexible-phase locking.

On the other hand, it is well known that the $\lambda-\mu$ system [10] has a explicitly written stable limit cycle. Moreover, coupling of the two systems can easily reproduce the phase difference of quarter period without the time delay and the phase shift increasing in proportion to the time delay. These correspond to a) and b).

In this work, by using the $\lambda-\mu$ system, we construct a simplified model such that it can structurally agree with the walking model in terms of a) and b). The constructed simplified model could enable to easily analyze quantitatively phase dynamics. Thus this study attempts to physically or physiologically interpret the mechanism of the flexible-phase locking.

This paper is organized as follows. First in Section 2, we survey the walking model [1], and see the model's phase relationship between CPG activity and Body motion. Next in Section 3, we introduce a simplified model composed of the $\lambda-\mu$ system. Through the analysis and computer simulations of the simplified model, we investigate theoretically the mechanisms of the flexible-phase locking. Lastly in Section 4, we discuss about the mechanisms.

This study reveals that, depending on pathways on which the time delay is involved, the time delay induces different effectiveness in direction of phase shift. That is, the time delay on afferent and efferent pathway induces the phase of CPG activity to shift forward and backward in proportion to the increase of time delay interval, respectively. Furthermore, this study reads to physical understanding of the condition 2), i.e., signs of the coupling coefficients in the simplified model [1]. That is, signs of the coupling coefficients correspond to the excitatory and inhibitory connection, which is interpreted to occur the forward and backward shift of the CPG activity, respectively.

2. The walking model

2.1. Walking model

In this section we introduce our walking model in which flexible-phase locking can occur [11]. We called this model *the delayed direct-coupled CPG and Body* (Fig. 1).

The time delays through the sensorimotor loop are assumed to be represented as follows: The total time delay Δ_t through the loop consists of two equivalent amounts of time delay $\Delta_t = \Delta_a + \Delta_e$, i.e., an afferent delay Δ_a and an efferent delay Δ_e [9, 12, 13].

First, we assume $\Delta_a = \Delta_e (=: \Delta)$.

The Body consists of an interconnected chain of 5 rigid links in the sagittal plane as shown in Fig. 7. The reaction forces from the ground are modeled as a two-dimensional spring and damper. The motion of the Body can be represented by differential equations of a (6×1) vector of mass point positions of 1 link and inertial angles of 4 links. The equations are derived by means of the Newton-Euler method (Appendix A).

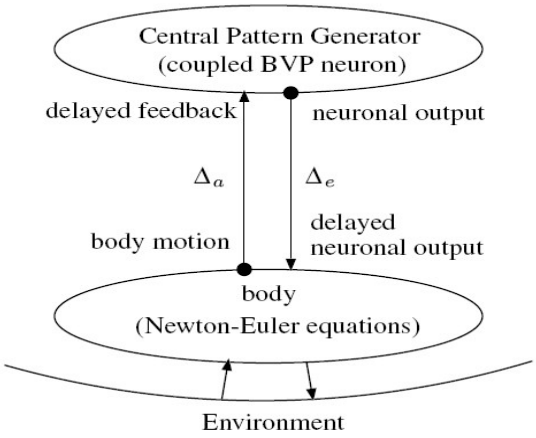

Fig. 1: Outline of the walking model (a delayed synaptically coupling of CPG and Body). Δ_a is the afferent time delay and Δ_e is the efferent time delay.

The CPG composed of 12 neurons (Fig. 2) is represented by the following BVP (Bonhöffer van del Pol) differential equations [14]:

$$\begin{cases} \tau_i \dot{u}_i(t) = u_i(t) - v_i(t) - u_i(t)^3/3 + \sum_{ij=1}^{12}(w_{ij}y_i) \\ \qquad\qquad +u_0 + \alpha_w F_i(\mathbf{x}(\mathrm{t}-\Delta)), \\ \tau_i' \dot{v}_i(t) = u_i(t) + a - b v_i(t), \end{cases} \tag{1}$$

where u_i is the potential of the ith neuron; v_i is responsible for the accommodation and refractoriness of the ith neuron; w_{ij} is the connecting weight from the ith neuron to the jth neuron; τ_i and τ_i' are the time constants of the potential and the accommodation and refractory effects, respectively; y_i is the output of the ith neuron; u_0 is the constant parameter. α_w is a positive coefficient of afferent connections from the Body to the CPG; F_i is a sensory feedback, and $\mathbf{x}$ is a (6×1) vector of the mass point positions of 1 link and the inertial angles of 4 links (Fig. 7); t is the time; a and b are positive constants; the natural frequency of each joint neuron (τ_i, τ_i') is set a value similar to the natural frequency of each joint angle [15].

It is well known that a BVP potential has an asymptotically stable limit cycle attractor with appropriate parameters [14], which was confirmed by computer simulation.

Torque was assumed to be proportional to the magnitude of the neuronal output. This periodic torque causes the Body to oscillate harmonically. At the same time, the outputs of the hip joint's flexor neurons (1st and 7th) control the mechanical impedance (muscle viscoelasticity) of the hip joint so that the maximum angle of the thigh can be voluntarily and approximately confined Eq. (16). Consequently, this impedance control can stabilize the orbit of the Body oscillation induced by the periodic torque. Thus, the Body oscillation could also be characterized by a limit

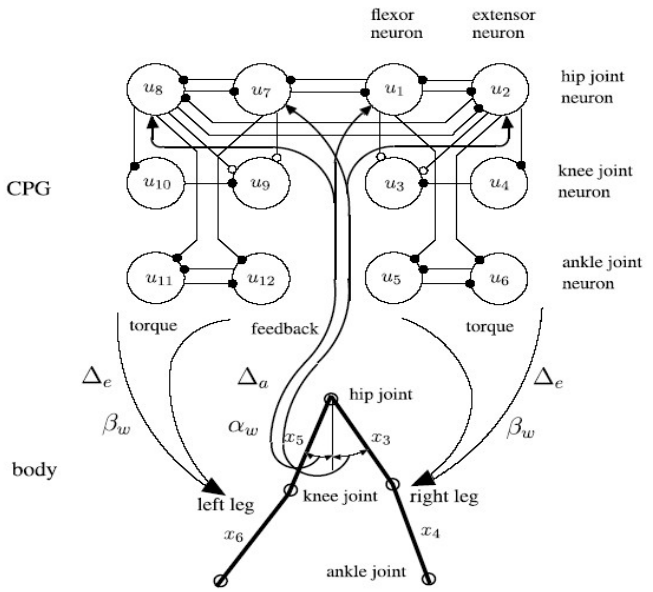

Fig. 2: Central pattern generator (CPG) and feedback pathway. u_i is the potential of the ith neuron in the CPG. ∘ and • denote an excitatory connection and an inhibitory connection, respectively. x_3, x_4, x_5, and x_6 are the angles of Body segments. The motion of the hip,the knee joint and the ankle joint in the right leg are governed by neurons 1-2, 3-4, and 5-6, respectively. Similarly, the motion of the joints in the left leg is governed by neurons 7-12. Odd-numbered neurons control flexion of the joint, while even-numbered neurons control its extension. The hip joint angles of both legs are used as feedback to the hip joint neurons. The afferent delay Δ_a and the efferent delay Δ_e take place in the transmission of the neuronal output and of the feedback, respectively. α_w and β_w are the afferent coupling strength and the efferent coupling strength. It is confirmed by computer simulation that the CPG itself has an asymptotically stable limit cycle.

cycle.

The CPG receives sensory feedback from the Body. The feedback F_i, $i = 1, \ldots, 12$, to the ith neuron is given as follows:

$$F_1 = F, \;\; F_2 = F', \;\; F_7 = F', \;\; F_8 = F, \;\; F_i = 0 \text{ (else)},$$

where F, F' are given as follows:

$$F = -f(-x_5(t-\Delta)), \;\; F' = -f(-x_3(t-\Delta)),$$
$$f(x) = \max(0, x),$$

where x_3 and x_5 are the thigh angles of the right and left legs at the hip joint, respectively, as defined in Appendix A.

2.2. Simulation results

The loop time delay Δ_t was the only selected simulation parameter. The other parameters were fixed to a certain value.

For $\Delta_t = 0$ ms, the model resulted in a stable walking pattern. Our result also shows that the Body oscillation can be characterized by a stable limit cycle.

For a loop delay $\Delta_t > 0$, our model clearly showed an ability to generate a stable walking pattern similar to that

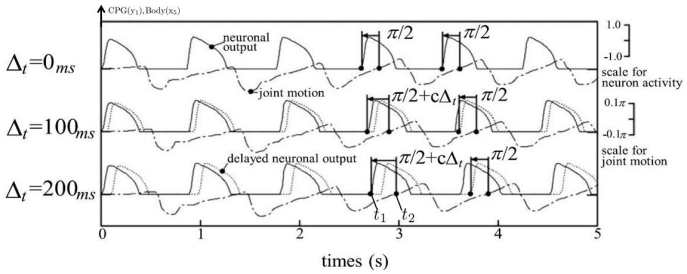

Fig. 3: Flexible-phase locking of neuron activity in the walking model. The graph shows the activities of flexor neuron (y_1) and angle motion (x_5) in the left leg. Solid line, dotted line, and dot-dashed line denote the neuronal output, the delayed neuronal output, and the joint angle motion, respectively. Arrows indicate the phase difference between neuronal output and joint angle motion, and between delayed neuronal output and joint angle motion, taking as reference the time when the joint angle becomes larger than 0. The phase of neuronal output is shifted forward according to Δ_t; t_1, t_2 are the times, c represents a constant value. Therefore, the phase relationship between delayed neuronal output and joint angle motion is maintained constant.

in the case of no delay. Fig. 3 shows the hip neuronal output y_1, the delayed neuronal output, and the hip joint angle x_5 simulated under three conditions of Δ_t; $\Delta_t = 0$, 100, and 200 ms.

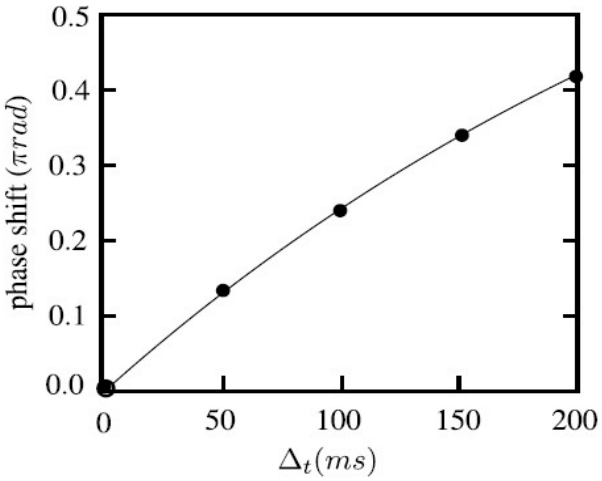

Fig. 4: The graph shows the forward phase shift of neuronal output as a function of the total time delay Δ_t. The vertical axis denotes $\frac{t_2 - t_1}{T} - \frac{\pi}{2}$. T is a period of walking cycle. The phase of neuronal output is shifted forward according to Δ_t.

As showed in Fig. 3, the phase of the neuronal output could shift forward on that of the joint motion according to Δ_t; When $\Delta_t = 0$, the phase shift of neuronal output shifted $\pi/2$ ahead of the joint motion; besides, this phase shift increases in proportion to the increase of Δ_t (see Fig. 4). Therefore, the phase relationship between the delayed neuronal output and the joint angle is constantly maintained in spite of changes of Δ_t.

The computer simulations showed the phase behaviors

between the CPG activity and the Body motion under the condition of $\Delta_a = \Delta_e$ in Fig. 3, 4.

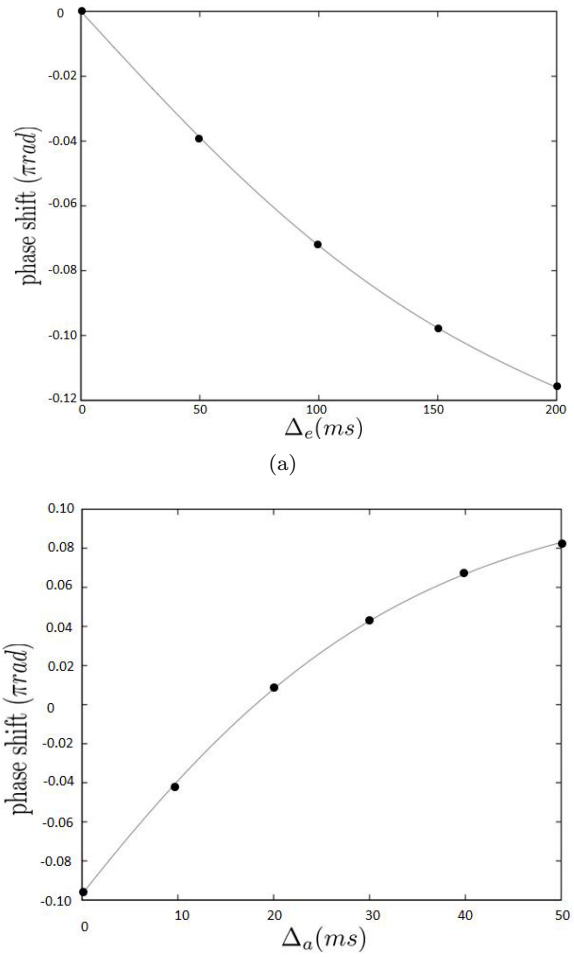

Fig. 5: The graph shows the forward phase shift of neuronal output as a function of the afferent time delay Δ_a and the backward of joint angle motion as a function of the efferent time delay Δ_e. The vertical axis denotes $\frac{t_2 - t_1}{T} - \frac{\pi}{2}$. T is a period of walking cycle. The phase of neuronal output is shifted forward according to Δ_t. (a) shows the relationship between phase shift and the efferent time delay Δ_e when $\Delta_a = 0$. The phase shift decreased in proportion to the increase of Δ_e (b) shows the relationship between phase shift and the afferent time delay Δ_a when $\Delta_e = 50\,\text{ms}$. The phase shift increased in proportion to the increase of Δ_a.

When $\Delta_a \neq \Delta_e$, as the computer simulations showed in Fig. 5, the phase shift is increasing or decreasing with respect to Δ_a, Δ_e. It shows the relationships between the phase shift and the efferent time delay Δ_e when $\Delta_a = 0\,\text{ms}$, and the relationships between the phase shift and the efferent time delay Δ_a when $\Delta_e = 50\,\text{ms}$. In relation to such a phase shift, the computer simulations showed that the phase shift increases in proportion to the increase of the time delay Δ_a; conversely, the phase shift decreases in proportion to the increase of the time delay Δ_e, which corresponds to the elemental effectiveness of the flexible-phase locking.

3. Analysis of the walking model

In the previous section, we showed a proper phase relationship between the CPG activity and the Body motion (Fig. 5). In this section, we will give a theoretical understanding of the phase shift according to time delays Δ_a and Δ_e by introducing the $\lambda - \mu$ system [10] as a simplified model and analyzing it.

As we see, the walking model can be regarded as a coupling of two oscillators, we limit our analysis to a simplified model consisting of two stable oscillators as shown in Fig. 6.

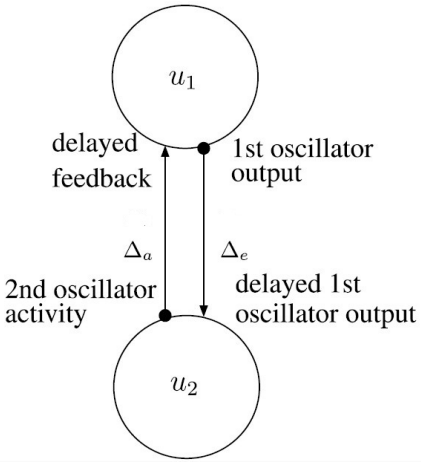

Fig. 6: The conceptual diagram of the simplified model. $\boldsymbol{u_1}$ and $\boldsymbol{u_2}$ are the potentials of the 1st neurons and the 2nd neurons. The connections from the CPG to the Body are inhibitory and the connections from the Body to the CPG are excitatory.

In the walking model, the connections from CPG to Body are inhibitory and the connections from the Body to the CPG are excitatory. The simplified model with synaptic coupling considered in this section is

$$\begin{cases} \dot{\boldsymbol{u_1}} = G(\boldsymbol{u_1}) + \varepsilon \boldsymbol{A_1 u_2}(t - \Delta_e), \\ \dot{\boldsymbol{u_2}} = G(\boldsymbol{u_2}) + \varepsilon \boldsymbol{A_2 u_1}(t - \Delta_a), \end{cases} \tag{2}$$

where $0 < \varepsilon \ll 1$ and the vectors $\boldsymbol{u_1}$, $\boldsymbol{u_2}$ and $G(\boldsymbol{u})$ are defined by

$$\boldsymbol{u_1} := \begin{pmatrix} x_1 \\ y_1 \end{pmatrix}, \boldsymbol{u_2} := \begin{pmatrix} x_2 \\ y_2 \end{pmatrix}$$

and

$$G(\boldsymbol{u}) := \begin{pmatrix} (\lambda - x^2 - y^2)x - \mu y \\ (\lambda - x^2 - y^2)x + \mu x \end{pmatrix}$$

for positive constants $\lambda > 0$ and $\mu > 0$. Matrices A_1, A_2 are

$$\boldsymbol{A_1} = \begin{pmatrix} a_{11} & a_{12} \\ a_{21} & a_{22} \end{pmatrix}, \quad \boldsymbol{A_2} = \begin{pmatrix} b_{11} & b_{12} \\ b_{21} & b_{22} \end{pmatrix}.$$

Here, we consider that the 1st oscillator $\boldsymbol{u_1}$ and the 2nd oscillator $\boldsymbol{u_2}$ correspond to CPG and Body of the walking model, respectively. ε is a small coupling strength coefficient of the synapse connections. $\boldsymbol{A_1}$, $\boldsymbol{A_2}$ are the (2×2) coupling matrices. Δ_a, Δ_e are the time delay from Body to CPG and CPG to Body, respectively.

3.1. Limit Cycle

First, we consider the unperturbed system of $\varepsilon = 0$ in (2)

$$\dot{\boldsymbol{u}} = G(\boldsymbol{u}), \quad \boldsymbol{u} \in \boldsymbol{R}^2, \tag{3}$$

where, the vectors $\boldsymbol{u}, G(\boldsymbol{u}) \in \boldsymbol{R}^2$ are defined by

$$\boldsymbol{u} = \begin{pmatrix} x \\ y \end{pmatrix}, \quad G(\boldsymbol{u}) = \begin{pmatrix} (\lambda - x^2 - y^2)x - \mu y \\ (\lambda - x^2 - y^2)x + \mu x \end{pmatrix}$$

for positive constants $\lambda > 0$ and $\mu > 0$. It is easy to see that (3) has a periodic solution $S(t) := \sqrt{\lambda}(\cos \mu t, \sin \mu t)$ with a period $p := 2\pi/\mu$.

We now check the stability of the periodic solution $S(t)$ in (3). Let $A(t)$ be the linearized matrix with respect to $S(t)$, that is,

$$\begin{aligned} A(t) &:= \frac{\partial \boldsymbol{G}}{\partial \boldsymbol{u}}(S(t)) \\ &= \begin{pmatrix} -2\lambda \cos^2 \mu t & -2\lambda \cos \mu t \sin \mu t - \mu \\ -2\lambda \cos \mu t \sin \mu t + \mu & -2\lambda \sin^2 \mu t \end{pmatrix}. \end{aligned}$$

Proposition 1 (Ei [16])**.** *The periodic solution $S(t)$ is asymptotically stable in* (3)*.*

Proof. We consider the fundamental matrix

$$\boldsymbol{Y}(t) = (\boldsymbol{v_1}(t), \boldsymbol{v_2}(t)) \text{ for } \boldsymbol{v_1}, \boldsymbol{v_2} \in \boldsymbol{R}^2$$

of the linearized ODE

$$\dot{\boldsymbol{Y}}(t) = A(t)\boldsymbol{Y}(t).$$

$\boldsymbol{v_1}$ is obtained as the derivative of $S(t)$

$$\boldsymbol{v_1}(t) = \dot{S} = \sqrt{\lambda}\mu(-\sin \mu t, \cos \mu t).$$

$\boldsymbol{v_2}$ is obtained by putting

$$\boldsymbol{v_2}(t) = \begin{pmatrix} -u(t) \sin \mu t \\ v(t) \cos \mu t \end{pmatrix}.$$

Then $\dot{\boldsymbol{v_2}} = A(t)\boldsymbol{v_2}$ yields

$$\begin{cases} -\mu \dot{u} \sin \mu t - \mu^2 u \cos \mu t = (-2\cos^2 \mu t)(-\mu u \sin \mu t) \\ \qquad\qquad + (-2 \cos \mu t \sin \mu t - \mu)\mu v \cos \mu t, \\ \mu \dot{v} \cos \mu t - \mu^2 v \sin \mu t = (-2 \sin^2 \mu t)\mu v \cos \mu t \\ \qquad\qquad + (-2 \cos \mu t \sin \mu t + \mu)(-\mu u \sin \mu t), \end{cases}$$

which is

$$\begin{cases} \dot{u} = \left(\mu \dfrac{\cos \mu t}{\sin \mu t} + 2\cos^2 \mu t\right)(v - u), \\ \dot{v} = \left(\mu \dfrac{\sin \mu t}{\cos \mu t} - 2\sin^2 \mu t\right)(v - u). \end{cases} \tag{4}$$

It follows that

$$\dot{w} = \left(\mu \frac{\sin \mu t}{\cos \mu t} - \mu \frac{\cos \mu t}{\sin \mu t} - 2\right) w \tag{5}$$

by using the change of variable $w := v - u$. Then w is obtained in the form

$$\begin{aligned} w &= \exp\left(\int \left(\mu \frac{\sin \mu t}{\cos \mu t} - \mu \frac{\cos \mu t}{\sin \mu t} - 2\right) dt\right) \\ &= \frac{1}{\cos \mu t \sin \mu t} e^{-2t}. \end{aligned}$$

Substituting $w = v - u$ into (4) and (5), we have

$$\begin{aligned} \dot{u}(t) &= \left(\mu \frac{\cos \mu t}{\sin \mu t} + 2\cos^2 \mu t\right) \frac{1}{\cos \mu t \sin \mu t} e^{-2t} \\ &= \frac{(\mu + 2 \cos \mu t \sin \mu t)}{\sin^2 \mu t} e^{-2t} \end{aligned}$$

and hence

$$u(t) = \int \frac{\mu t + 2 \cos \mu t \sin \mu t}{\sin^2 \mu t} e^{-2t} dt = -\frac{\cos \mu t}{\sin \mu t} e^{-2t}.$$

Similarly, we can get

$$v(t) = \int \frac{\mu t + 2 \cos \mu t \sin \mu t}{\sin^2 \mu t} e^{-2t} dt = \frac{\cos \mu t}{\sin \mu t} e^{-2t}.$$

Thus, the fundamental matrix $Y(t)$ is given by

$$Y(t) = \begin{pmatrix} -\sqrt{\lambda}\mu \sin \mu t & e^{-2t} \cos \mu t \\ \sqrt{\lambda}\mu \cos \mu t & e^{-2t} \sin \mu t \end{pmatrix}.$$

It is easy to check that

$$Y^{-1}(0) = \begin{pmatrix} 0 & \frac{1}{\sqrt{\lambda}\mu} \\ 1 & 0 \end{pmatrix}, \quad Y\left(\frac{2\pi}{\mu}\right) = \begin{pmatrix} 0 & e^{\frac{-4\pi}{\mu}} \\ \sqrt{\lambda}\mu & 0 \end{pmatrix}.$$

Then the periodic map U is calculated as

$$U = Y(2\pi/\mu)Y^{-1}(0) = \begin{pmatrix} e^{-4\pi/\mu} & 0 \\ 0 & 1 \end{pmatrix},$$

which implies the two floquet multipliers are 1 and $e^{-4\pi/\mu} < 1$ and the periodic solution $S(t)$ is asymptotically stable in (3). □

Let

$$\boldsymbol{X}_P := \{\boldsymbol{v} \in C[0, p]; \boldsymbol{v}(0) = \boldsymbol{v}(p)\}$$

and

$$\langle \boldsymbol{u}, \boldsymbol{v} \rangle_P := \int_0^p \langle \boldsymbol{u}(t), \boldsymbol{v}(t) \rangle dt.$$

L be the linearized operator with respect to the periodic solution $S(t)$, that is

$$L\boldsymbol{v} := G'(S(t))\boldsymbol{v} - \boldsymbol{v}_t \text{ for } \boldsymbol{v} \in \boldsymbol{X}_P.$$

L^* is the adjoint operator of L with respect to the inner product. L^* is given by

$$L^* = {}^tG'(S(t)) + \partial_t.$$

Especially, 0 is a simple eigenvalue of L because $S(t)$ is linearly stable. Hence there exists an eigenfunction $\phi^*(t) \in \boldsymbol{X}_P$ such that $L^*\phi^* = 0$ and $\langle S_t(t), \phi^* \rangle_P = 1$.

Proposition 2. *The eigenfunction ϕ^* is given by*

$$\phi^*(t) = \frac{1}{2\pi\sqrt{\lambda}} \begin{pmatrix} -\sin \mu t \\ \cos \mu t \end{pmatrix}.$$

Proof. First, we write $\phi^*(t)$ as

$$\phi^*(t) = \begin{pmatrix} U(t) \\ V(t) \end{pmatrix}.$$

Since the adjoint operator of L is expressed by

$$L^* = {}^tG'(S(t)) + \partial_t,$$

ϕ^* satisfies

$$L^*\phi^* = {}^tG'(S(t))\phi^* + \partial_t\phi^* = 0 \tag{6}$$

with $\langle S_t(t), \phi^* \rangle_P = 1$.

Here we have

$$G'(S(t)) = \begin{pmatrix} -2\lambda\cos^2 \mu t & -2\lambda\cos\mu t\sin\mu t - \mu \\ -2\lambda\cos\mu t\sin\mu t + \mu & -2\lambda\sin^2\mu t \end{pmatrix}$$

and

$${}^tG'(S(t)) = \begin{pmatrix} -2\lambda\cos^2 \mu t & -2\lambda\cos\mu t\sin\mu t + \mu \\ -2\lambda\cos\mu t\sin\mu t - \mu & -2\lambda\sin^2\mu t \end{pmatrix}$$

Therefore (6) becomes

$$\begin{pmatrix} -2\lambda\cos^2 \mu t & -2\lambda\cos\mu t\sin\mu t + \mu \\ -2\lambda\cos\mu t\sin\mu t - \mu & -2\lambda\sin^2\mu t \end{pmatrix} \begin{pmatrix} U(t) \\ V(t) \end{pmatrix} + \partial_t \begin{pmatrix} U(t) \\ V(t) \end{pmatrix} = 0$$

with

$$\int_0^{\frac{2\pi}{\mu}} (-\sqrt{\lambda}\mu \sin \mu t U(t) + \sqrt{\lambda}\mu \cos \mu t V(t))dt = 1.$$

That is,

$$\begin{cases} -2U(t)\cos^2 \mu t + (-2\sin\mu t\cos\mu t + \mu)V(t) + \dot{U}(t) = 0, \\ -2V(t)\sin^2 \mu t + (-2\sin\mu t\cos\mu t - \mu)U(t) + \dot{V}(t) = 0, \\ -\sqrt{\lambda}\sin\mu t U(t) + \sqrt{\lambda}\cos\mu t V(t) = 1/2\pi. \end{cases}$$

which can be solved as

$$\begin{cases} U(t) = -\dfrac{1}{2\pi\sqrt{\lambda}}\sin\mu t, \\ V(t) = \dfrac{1}{2\pi\sqrt{\lambda}}\cos\mu t, \end{cases}$$

and we have

$$\phi^*(t) = \frac{1}{2\pi\sqrt{\lambda}} \begin{pmatrix} -\sin \mu t \\ \cos \mu t \end{pmatrix}. \qquad \square$$

3.2. Phase dynamics

In the case $\varepsilon > 0$ is sufficiently small but not 0, the solution of (2) can be regarded as follows

$$\boldsymbol{u_1}(t) = S(t+h_1(t)) + o(1),\ \boldsymbol{u_2}(t) = S(t+h_2(t)) + o(1),\ \varepsilon \downarrow 0$$

and hence $\boldsymbol{u_1}(t-\Delta_a), \boldsymbol{u_2}(t-\Delta_e)$ is close to

$$\boldsymbol{u_1}(t-\Delta_a) \sim S(t-\Delta_a+h_1(t)),\ \boldsymbol{u_2}(t-\Delta_e) \sim S(t-\Delta_e+h_2(t)).$$

Here we define $h_1 = h_1(t)$ and $h_2 = h_2(t)$ are the phases of the 1st oscillator $\boldsymbol{u_1}$ and the 2nd oscillator $\boldsymbol{u_2}$, respectively. The phase difference $h(t)$ is defined by

$$h(t) := h_2(t) - h_1(t).$$

Proposition 3 (Ei [16])**.** *$|\boldsymbol{u}_j(t) - S(t+h_j(t))| \le O(\varepsilon)$ hold and $h_1(t)$, $h_2(t)$ satisfy*

$$\dot{h_1}(t) = \varepsilon\omega_1(h) + O(\varepsilon^2), \quad \dot{h_2}(t) = \varepsilon\omega_2(h) + O(\varepsilon^2),$$

where

$$\omega_1(h) := \int_0^p \langle \boldsymbol{A_1} S(t - \Delta_e + h_2), \phi^*(t + h_1)\rangle dt,$$

$$\omega_2(h) := \int_0^p \langle \boldsymbol{A_2} S(t - \Delta_a + h_1), \phi^*(t + h_2)\rangle dt.$$

Here, $\omega_1(h)$ can be represented in the form

$$\omega_1(h) = \int_0^p \langle \boldsymbol{A_1} S(z + h - \Delta_e), \phi^*(z)\rangle dz$$

by changing the variable $z := t + h_1$. Similarly, $\omega_2(h)$ can also be written as

$$\omega_2(h) = \int_0^p \langle \boldsymbol{A_2} S(z - h - \Delta_a), \phi^*(z)\rangle dz.$$

Proposition 4. *$\omega_1(h)$, $\omega_2(h)$ are calculated as follows:*

$$\omega_1(h) = \frac{a_{21} - a_{12}}{2\sqrt{\lambda}\mu}\cos\mu(h - \Delta_e) + \frac{a_{22} + a_{11}}{2\sqrt{\lambda}\mu}\sin\mu(h - \Delta_e),$$

$$\omega_2(h) = \frac{b_{21} - b_{12}}{2\sqrt{\lambda}\mu}\cos\mu(h + \Delta_a) - \frac{b_{22} + b_{11}}{2\sqrt{\lambda}\mu}\sin\mu(h + \Delta_a).$$

Proof. We can calculate

$$\begin{aligned} \omega_1(h) &= \int_0^p \langle \boldsymbol{A_1} S(z + h - \Delta_e), \phi^*(z)\rangle dz \\ &= \int_0^{\frac{2\pi}{\mu}} \langle \boldsymbol{A_1} \begin{pmatrix} \cos\mu(z + h - \Delta_e) \\ \sin\mu(z + h - \Delta_e) \end{pmatrix}, \phi^*(z)\rangle dz \\ &= \int_0^p \langle \boldsymbol{A_1} \cos\mu(h - \Delta_e) \begin{pmatrix} \cos\mu z \\ \sin\mu z \end{pmatrix}, \phi^*(z)\rangle dz \\ &\quad + \boldsymbol{A_1} \sin\mu(h - \Delta_e) \begin{pmatrix} -\sin\mu z \\ \cos\mu z \end{pmatrix}, \phi^*(z)\rangle dz \\ &= \cos\mu(h - \Delta_e) \int_0^p \langle \boldsymbol{A_1} \begin{pmatrix} \cos\mu z \\ \sin\mu z \end{pmatrix}, \phi^*(z)\rangle dz \\ &\quad + \sin\mu(h - \Delta_e) \int_0^p \langle \boldsymbol{A_1} \begin{pmatrix} -\sin\mu z \\ \cos\mu z \end{pmatrix}, \phi^*(z)\rangle dz \\ &= \cos\mu(h - \Delta_e)\frac{a_{21} - a_{12}}{2\sqrt{\lambda}\mu} + \sin\mu(h - \Delta_e)\frac{a_{22} + a_{11}}{2\sqrt{\lambda}\mu}. \end{aligned}$$

Thus $\omega_1(h)$ is given in the form

$$\omega_1(h) = \frac{a_{21} - a_{12}}{2\sqrt{\lambda}\mu} \cos\mu(h - \Delta_e) + \frac{a_{22} + a_{11}}{2\sqrt{\lambda}\mu} \sin\mu(h - \Delta_e).$$

Similarly, we also can get

$$\omega_2(h) = \frac{b_{21} - b_{12}}{2\sqrt{\lambda}\mu} \cos\mu(h + \Delta_a) - \frac{b_{22} + b_{11}}{2\sqrt{\lambda}\mu} \sin\mu(h + \Delta_a).$$

□

Here, we define

$$\begin{cases} M_1 := a_{21} - a_{12}, & N_1 := a_{11} + a_{22}, \\ M_2 := b_{21} - b_{12}, & N_2 := b_{11} + b_{22}. \end{cases}$$

Then $\omega_1(h)$, $\omega_2(h)$ are represented as follows:

$$\omega_1(h) = \frac{\cos\mu(h - \Delta_e)}{2\sqrt{\lambda}\mu} M_1 + \frac{\sin\mu(h - \Delta_e)}{2\sqrt{\lambda}\mu} N_1,$$
$$\omega_2(h) = \frac{\cos\mu(h + \Delta_a)}{2\sqrt{\lambda}\mu} M_2 - \frac{\sin\mu(h + \Delta_a)}{2\sqrt{\lambda}\mu} N_2.$$

From Proposition 3, $\dot{h}_1(t)$, $\dot{h}_2(t)$ can be rewritten as

$$\begin{aligned} \dot{h_1}(t) &= \varepsilon\omega_1(h) + O(\varepsilon^2) \\ &= \varepsilon\frac{\cos\mu(h - \Delta_e)}{2\sqrt{\lambda}\mu} M_1 + \varepsilon\frac{\sin\mu(h - \Delta_e)}{2\sqrt{\lambda}\mu} N_1 + O(\varepsilon^2) \\ \dot{h_2}(t) &= \varepsilon\omega_2(h) + O(\varepsilon^2) \\ &= \varepsilon\frac{\cos\mu(h + \Delta_a)}{2\sqrt{\lambda}\mu} M_2 - \varepsilon\frac{\sin\mu(h + \Delta_a)}{2\sqrt{\lambda}\mu} N_2 + O(\varepsilon^2) \end{aligned} \tag{7}$$

and the phase difference $h(t)$ is given

$$\begin{aligned} \dot{h}(t) &:= \dot{h}_2(t) - \dot{h}_1(t) = \varepsilon(\omega_2(h) - \omega_1(h)) + O(\varepsilon^2) \\ &= \frac{\varepsilon}{2\sqrt{\lambda}\mu}(M_2 \cos\mu(h + \Delta_a) - N_2 \sin\mu(h + \Delta_a) \\ &\quad - M_1 \cos\mu(h - \Delta_e) - N_1 \sin\mu(h - \Delta_e)) + O(\varepsilon^2) \end{aligned} \tag{8}$$

3.3. Corresponding to walking model

In this subsection, we will determine the parameters M_1, M_2, N_1, N_2 so that our simplified model (2) can structurally correspond with the walking model (1). We omit higher order terms $O(\varepsilon)$ in (8).

3.3.1. Excitation and inhibition

As mentioned in previous section, the efferent and afferent pathway, i.e., the connection from CPG to Body and from Body to CPG is inhibitory and excitatory, respectively, in the walking model. We understand that the phase of CPG will speed up and the phase of Body will slow down, respectively. When both time delays $\Delta_a = \Delta_e = 0$, that is, we understand $\dot{h}_1(0) = \varepsilon\omega_1(0) > 0$ and $\dot{h}_2(0) = \varepsilon\omega_2(0) < 0$ by (7).

When $\Delta_a = \Delta_e = 0$, we have

$$\omega_1(0) = \frac{1}{2\mu} M_1 \text{ and } \omega_2(0) = \frac{1}{2\mu} M_2,$$

which means $M_1 > 0$ and $M_2 < 0$. Thus we assume

H1) $\qquad M_1 > 0 \text{ and } M_2 < 0.$

3.3.2. CPG phase quarter period ahead of Body phase

Since, $\dot{h}(t) = \dot{h}_2(t) - \dot{h}_1(t)$ can be written as

$$\begin{aligned} \dot{h}(t) &= \varepsilon\frac{\cos\mu h}{2\sqrt{\lambda}\mu}(M_2 - M_1) - \varepsilon\frac{\sin\mu h}{2\sqrt{\lambda}\mu}(N_2 + N_1) \\ &= \frac{\varepsilon}{2\sqrt{\lambda}\mu}\sqrt{(M_2 - M_1)^2 + (N_1 + N_2)^2}\cos(\mu h + \gamma_0). \end{aligned}$$

where

$$\begin{aligned} \cos\gamma_0 &= \frac{M_2 - M_1}{\sqrt{(M_2 - M_1)^2 + (N_1 + N_2)^2}}, \\ \sin\gamma_0 &= \frac{N_1 + N_2}{\sqrt{(M_2 - M_1)^2 + (N_1 + N_2)^2}}, \end{aligned} \tag{9}$$

the phase shift satisfies

$$h(t) \to \frac{\pi}{2\mu} - \frac{\gamma_0}{\mu} = \frac{1}{4}p - \frac{\gamma_0}{\mu} \text{ as } t \longrightarrow +\infty. \tag{10}$$

As mentioned in Section 2, the CPG phase is $p/4$ ahead of the Body phase when no time delays $\Delta_a = \Delta_e = 0$ in the walking model. In order to correspond with it, the phase difference (10) should satisfy

$$\frac{p}{4} - \frac{\gamma_0}{\mu} = -\frac{p}{4}.$$

Since $p = \dfrac{2\pi}{\mu}$ and $\dfrac{1}{4}p = \dfrac{\pi}{2\mu}$, we should assume $\gamma_0 = \pi$, that is

H2) $\qquad N_1 + N_2 = 0$

from (9).

3.4. Analysis of the phase shift

Under assumptions H1) and H2), we consider the effect of time delays Δ_a and Δ_e. From (8) and H1), H2), we have

$$\dot{h}(t) = \frac{\epsilon}{2\sqrt{\lambda}\mu}(\alpha\cos\mu h + \beta\sin\mu h), \tag{11}$$

where

$$\begin{aligned} \alpha &:= \alpha(\Delta_a, \Delta_e) \\ &= M_2 - N_2\mu\Delta_a - M_1 + N_1\mu\Delta_e + O(\Delta_a^2 + \Delta_e^2) \\ \beta &:= \beta(\Delta_a, \Delta_e) \\ &= -M_2\mu\Delta_a - N_2 - M_1\mu\Delta_e - N_1 + O(\Delta_a^2 + \Delta_e^2) \end{aligned}$$

by the expansions

$$\begin{cases} \cos\mu(h+\Delta_a) = \cos\mu h - \mu\Delta_a \sin\mu h + O(\Delta_a^2), \\ \sin\mu(h+\Delta_a) = \sin\mu h + \mu\Delta_a \cos\mu h + O(\Delta_a^2), \\ \cos\mu(h-\Delta_e) = \cos\mu h + \mu\Delta_e \sin\mu h + O(\Delta_e^2), \\ \sin\mu(h-\Delta_e) = \sin\mu h - \mu\Delta_e \cos\mu h + O(\Delta_e^2) \end{cases}$$

for $|\Delta_a|, |\Delta_e| \ll 1$. Then (11) reads

$$\dot{h}(t) = \frac{\varepsilon}{2\sqrt{\lambda}\mu}(\alpha^2+\beta^2)^{\frac{1}{2}}(\sin\mu h + \gamma), \tag{12}$$

where

$$\cos\gamma = \frac{\beta}{(\alpha^2+\beta^2)^{\frac{1}{2}}}, \quad \sin\gamma = \frac{\alpha}{(\alpha^2+\beta^2)^{\frac{1}{2}}}.$$

That is, the angle γ is given by

$$\gamma = \gamma(\Delta_a, \Delta_e) = \arccos\frac{\beta}{(\alpha^2+\beta^2)^{\frac{1}{2}}}.$$

Proposition 5.

$$\gamma(\Delta_a, \Delta_e) = -\frac{\pi}{2} + C_1\Delta_a + C_2\Delta_e + O(\Delta_a^2 + \Delta_e^2) \tag{13}$$

holds for $|\Delta_a|, |\Delta_e| \ll 1$*, where*

$$C_1 := \frac{\mu M_2}{M_2 - M_1} > 0, \; C_2 := \frac{\mu M_1}{M_2 - M_1} < 0.$$

Proof. Seeing $\gamma(0,0) = -\frac{\pi}{2}$, we expand $\gamma(\Delta_a, \Delta_e)$ as

$$\begin{aligned} \gamma(\Delta_a, \Delta_e) &= \gamma(0,0) + \frac{\partial\gamma(0,0)}{\partial\Delta_a}\Delta_a + \frac{\partial\gamma(0,0)}{\partial\Delta_e}\Delta_e \\ &\quad + O(\Delta_a^2 + \Delta_e^2) \\ &= -\frac{\pi}{2} + C_1\Delta_a + C_2\Delta_e + O(\Delta_a^2 + \Delta_e^2), \end{aligned}$$

when $|\Delta_a|, |\Delta_e| \ll 1$, where

$$C_1 := \frac{\mu M_2}{M_2 - M_1} > 0, \; C_2 := \frac{\mu M_1}{M_2 - M_1} < 0. \qquad \square$$

Thus, we find from (12)

$$\mu h(t) + \gamma \to -\pi \;\text{ as }\; t \to +\infty.$$

From (13), we have

$$\mu h(t) - \frac{\pi}{2} + C_1\Delta_a + C_2\Delta_e \to -\pi$$

and therefore

$$h(t) \to -\pi/2\mu - \frac{C_1}{\mu}\Delta_a - \frac{C_2}{\mu}\Delta_e.$$

Thus the phase difference $h(t) = h_2(t) - h_1(t)$ with the period $p = 2\pi/\mu$ satisfies

$$\begin{aligned} h(t) \to -p/4 - \frac{C_1}{\mu}\Delta_a - \frac{C_2}{\mu}\Delta_e + O(\Delta_a^2 + \Delta_e^2) \\ (t \to +\infty) \end{aligned} \tag{14}$$

and

$$\begin{aligned} h_1(t) \to h_2(t) + p/4 + \frac{C_1}{\mu}\Delta_a + \frac{C_2}{\mu}\Delta_e \\ + O(\Delta_a^2 + \Delta_e^2) \quad (t \to +\infty) \end{aligned} \tag{15}$$

From (15), the phase of the 1st oscillator $\boldsymbol{u}_1$ could shift forward on that of the 2nd oscillator $\boldsymbol{u}_2$ according to the time delay Δ_a, Δ_e. Precisely speaking, the phase shift increases in proportion to Δ_a and the phase shift decreases in proportion to Δ_e. These observation quite well agree with the results of computer simulations of the walking model (1).

4. Discussions

The computer simulation results for the walking model (1) showed two typical properties that 1) the phase of the CPG activity shifted $p/4$ (p is a period) ahead of the Body motion when the loop time delay $\Delta_t = 0$ (Fig. 3), 2) the phase shift increases according to the increase of the afferent time delay Δ_a; conversely, the phase shift decreases according to the increase of the efferent time delay Δ_e as observed in (Fig. 5).

In order to understand these phenomena theoretically, we introduced the simplified model consisting of two coupled oscillators characterized by stable limit cycles. In that model, coefficients are adjusted such that typical properties a) and b) mentioned in Introduction are reappeared.

Under these conditions, we analyzed the simplified model by using the phase dynamical approach [16, 17] and the phase difference of the 1st oscillator $\boldsymbol{u}_1$ (CPG) and 2nd oscillator $\boldsymbol{u}_2$ (Body) were derived as

$$h(t) = h_2(t) - h_1(t) \to -p/4 - \frac{C_1}{\mu}\Delta_a - \frac{C_2}{\mu}\Delta_e, \; (t \longrightarrow +\infty)$$

where

$$\frac{C_1}{\mu} = \frac{M_1}{M_2 - M_1} < 0, \quad \frac{C_2}{\mu} = \frac{\mu M_2}{M_2 - M_1} > 0,$$

when time delays Δ_a and Δ_e exist. Thus, the phase difference $h(t)$ is increasing or decreasing with respect to Δ_a or Δ_e, respectively while phase of the 1st oscillator $\boldsymbol{u}_1$ (CPG) could shift ahead $p/4$ of the 2nd oscillator $\boldsymbol{u}_2$ (Body) in the case of no time delay. These analytical results quit agree with the simulation results in the walking model (1) (Fig. 4, 5). Thus, the effects against time delays (flexible-phase locking) can be completely and naturally reduced in our simplified model.

The previous study [1] has theoretically clarified the effectiveness against total time delay on a sensorimotor loop. This study revealed that, depending on pathways on which time delays Δ_a and Δ_e are involved, the time delay induces different effectiveness in direction of phase shift. Our research assumed only the connection of excitation and inhibition and the function forming a quarter phase difference, as mentioned as H1) and H2) in Sec. 3.3. Nevertheless, the flexible-phase locking was reproduced completely. This

strongly suggests that only the connection of excitation and inhibition and the function forming a quarter phase difference automatically yield the flexible-phase locking in general. This is an unexpected and surprising scientific discovery.

This study also reads to physical understanding of the condition 2), i.e., signs of the coupling coefficients in the simplified model [1]. Our analysis simply assumed the excitation and inhibition at connections to be a force of the forward and backward phase shift, respectively, as in H1). This means to need no alternative assumptions in order to gain the flexible-phase locking. Thus, the excitation and inhibition at connections can be interpreted as a force of the forward and backward phase shift.

Appendix A. The equations of motion for the Body of the walking model

All variables and conventions correspond to those shown in Fig. 7. All variables and parameters follow the ones proposed by Taga (1994). By using the Newton-Euler method, motion of the Body (Taga, 1991) can be written as follows:

$$P(\mathrm{x})\ddot{\mathrm{x}} = \mathrm{Q}(\mathrm{x}, \ddot{\mathrm{x}}, \mathrm{T_r}(\mathrm{y})),$$

therefore,

$$\ddot{\mathbf{x}} = [P(\mathbf{x})]^{-1}\mathrm{Q}(\mathrm{x}, \ddot{\mathrm{x}}, \mathrm{T_r}(\mathrm{y})),$$

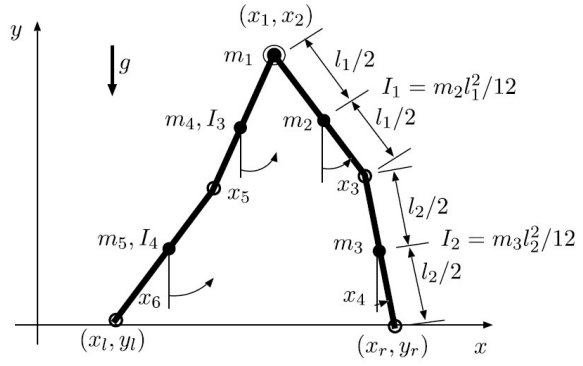

Fig. 7: Model of bipedal Body as an interconnected chain of 5 rigid links (a point mass m_1 on the hip and four rigid bodies $I_i (i = 1, 4)$

where

$$\mathbf{x} = \begin{pmatrix} x_1 \\ x_2 \\ x_3 \\ x_4 \\ x_5 \\ x_6 \end{pmatrix},$$

$p_{11} = \sum_{n=1}^{5} m_n,$
$p_{12} = 0,$
$p_{13} = (0.5m_2 + m_3)I_1 \cos(x_3),$
$p_{14} = 0.5m_3 l_2 \cos(x_4),$
$p_{15} = (0.5m_4 + m_5)l_3 \cos(x_5),$
$p_{16} = 0.5m_5 l_4 \cos(x_6),$
$p_{21} = 0,$
$p_{22} = \sum_{n=1}^{5} m_n,$
$p_{23} = (0.5m_2 + m_3)I_1 \sin(x_3),$
$p_{24} = 0.5m_3 l_2 \sin(x_4),$
$p_{25} = (0.5m_4 + m_5)l_3 \sin(x_5),$
$p_{26} = 0.5m_5 l_4 \sin(x_6),$
$p_{31} = (0.5m_2 + m_3)I_1 \cos(x_3),$
$p_{32} = (0.5m_2 + m_3)I_1 \sin(x_3),$
$p_{33} = 0.25m_2 l_1^2 + m_3 l_1^2 + I_1,$
$p_{34} = 0.5m_3 l_1 l_2 \cos(x_4 - x_3),$
$p_{35} = 0,$
$p_{36} = 0,$
$p_{41} = 0.5m_3 l_2 \cos(x_4),$
$p_{42} = 0.5m_3 l_2 \sin(x_4),$
$p_{43} = 0.5m_3 l_1 l_2 \cos(x_4 - x_3),$
$p_{44} = I_2 + 0.25m_3 l_2^2,$
$p_{45} = 0,$
$p_{46} = 0,$
$p_{51} = (0.5m_4 + m_5)I_3 \cos(x_5),$
$p_{52} = (0.5m_4 + m_5)I_3 \sin(x_5),$
$p_{53} = 0,$
$p_{54} = 0,$
$p_{55} = (0.25m_4 + m_5)l_3^2 + I_3,$
$p_{56} = 0.5m_5 l_3 l_4 \cos(x_6 - x_5),$
$p_{61} = 0.5m_5 l_4 \cos(x_6),$
$p_{62} = 0.5m_5 l_4 \sin(x_6),$
$p_{63} = 0,$
$p_{64} = 0,$
$p_{65} = 0.5m_5 l_3 l_4 \cos(x_5 - x_6),$
$p_{66} = 0.25m_5 l_4^2 + I_4,$

$$\begin{aligned} q_1 = {} & (0.5m_2 + m_3)l_1 \sin(x_3)\dot{x_3}^2 \\ & + 0.5m_3 l_2 \sin(x_4)\dot{x_4}^2 + (0.5m_4 + m_5)l_3 \sin(x_5)\dot{x_5}^2 \\ & + 0.5m_5 l_4 \sin(x_6)\dot{x_6}^2 + F_{g1} + F_{g3}, \end{aligned}$$

$$\begin{aligned} q_2 = {} & -(0.5m_2 + m_3)l_1 \cos(x_3)\dot{x_3}^2 - 0.5m_3 l_2 \cos(x_4)\dot{x_4}^2 \\ & -(0.5m_4 + m_5)l_3 \cos(x_5)\dot{x_5}^2 \\ & -0.5m_5 l_4 \sin(x_6)\dot{x_6}^2 + F_{g1} + F_{g2} - \sum_{n=1}^{5} m_n g, \end{aligned}$$

$$\begin{aligned} q_3 = {} & 0.5m_3 l_1 l_2 \sin(x_4 - x_3)\dot{x_4}^2 + F_{g1} l_1 \cos(x_3) \\ & + F_{g2} l_1 \sin(x_3) - (m_2 + 2m_3)0.5g l_1 \sin(x_3) \\ & + T_{rp1} + T_{r2} - T_{r2} - T_{r4}, \end{aligned}$$

$$
\begin{aligned}
q_4 &= 0.5m_3l_1l_2\sin(x_3-x_4)\dot{x_3}^2 - 0.5m_2gl_2\sin(x_4)\\
&\quad + F_{g1}l_2\cos(x_4) + F_{g2}l_2\cos(x_4)\\
&\quad + T_{rp2} + T_{r2} - T_{r3},\\
q_5 &= 0.5m_5l_3l_4\sin(x_6-x_5)\dot{x_6}^2\\
&\quad - 0.5(m_4+2m_5)gl_3\sin(x_5) + F_{g3}l_3\cos(x_5)\\
&\quad + F_{g4}l_3\sin(x_5) + T_{rp3} + T_{r4} - T_{r5} - T_{r1},\\
q_6 &= 0.5m_5l_3l_4\sin(x_5-x_6)\dot{x_5}^2 - 0.5m_4gl_4\sin(x_6)\\
&\quad + F_{g3}l_4\cos(x_6) + F_{g4}l_4\sin(x_6) + T_{rp4} + T_{r5} - T_{r6}.
\end{aligned}
$$

Horizontal and vertical forces on the ankles are given by

$$
F_{g1} = \begin{cases} -k_g(x_r - x_{r0}) - b_g\dot{x}_r & y_r - y_g(x_r) < 0,\\ 0 & \text{otherwise.}\end{cases}
$$

$$
F_{g2} = \begin{cases} -k_g(y_r - y_{r0}) + b_g f_1(-\dot{y}_r) & y_r - y_g(x_r) < 0,\\ 0 & \text{otherwise.}\end{cases}
$$

$$
F_{g3} = \begin{cases} -k_g(x_l - x_{l0}) - b_g\dot{x}_l & y_l - y_g(x_l) < 0,\\ 0 & \text{otherwise.}\end{cases}
$$

$$
F_{g4} = \begin{cases} -k_g(y_l - y_{l0}) + b_g f_1(-\dot{y}_l) & y_l - y_g(x_l) < 0,\\ 0 & \text{otherwise.}\end{cases}
$$

where $y_g(x)$ is the function which represents the terrain. When the ground is even, $y_g(x) = 0.(x_r, y_r)$ and (x_l, y_l) represent the positions of the ankles, which are given by

$$
\begin{aligned}
(x_r, y_r) &= (x_1 + l_1\cos x_3 + l_2\cos x_4, x_2 - l_1\sin x_3 - l_2\sin x_4),\\
(x_l, y_l) &= (x_1 + l_1\cos x_5 + l_2\cos x_6, x_2 - l_1\sin x_5 - l_2\sin x_6).
\end{aligned}
$$

Passively generated torques at each joint are given by

$$
\begin{aligned}
T_{rp1} &= k_r f_1(x_4 - x_3) - b_r f_2(x_4 - x_3)(x_4 - x_3)\\
&\quad - b(\dot{x}_3 - \dot{x}_5) - b(\dot{x}_3 - \dot{x}_4),\\
T_{rp2} &= -k_r f_1(x_4 - x_3) + b_r f_2(x_4 - x_3)(x_4 - x_3)\\
&\quad - b(\dot{x}_4 - \dot{x}_3) - b\dot{x}_4,\\
T_{rp3} &= k_r f_1(x_6 - x_5) - b_r f_2(x_6 - x_5)(x_6 - x_5)\\
&\quad - b(\dot{x}_5 - \dot{x}_3) - b(\dot{x}_5 - \dot{x}_6),\\
T_{rp4} &= -k_r f_1(x_6 - x_5) + b_r f_2(x_6 - x_5)(x_6 - x_5)\\
&\quad - b(\dot{x}_6 - \dot{x}_5) - b\dot{x}_6,
\end{aligned}
$$

where k and b are the positive constants.

Actively generated torques at each joint are given by

$$
\begin{aligned}
T_{r1} &= \beta_w[p_1(y_1 - y_2)\\
&\quad + f_2(y_1)\{-p_e f_1(x_3 - x_5 - x_0)^2 - p_b(\dot{x_3} - \dot{x_5})\}\\
T_{r2} &= \beta_w p_1(y_3 - y_4),\\
T_{r3} &= \beta_w(p_2 y - 3 - p_3 y_4) f_2(F_{g2}),\\
T_{r4} &= \beta_w[p_1(y_7 - y_8)\\
&\quad + f_2(y_7)\{-p_e f_1(x_5 - x_3 - x_0)^2 - p_b(\dot{x_5} - \dot{x_3})\}\\
T_{r5} &= \beta_w p_1(y_9 - y_{10}),\\
T_{r6} &= \beta_w p_2(y_1 1 - p_3 y_1 2) f_2(F_{g4}),
\end{aligned}
\tag{16}
$$

where β_w and p are the positive constants; depending on the ith neuronal output y_i, the mechanical viscoelastic torque at the hip joint was assumed to be produced when the hip joint angle between the left and right thighs was beyond a threshold angle x_0.

Besides

$$
f_1(z) = \max(0, z), \quad f_2(z) = \begin{cases} 0, & \text{for } z \le 0,\\ 1, & \text{otherwise.}\end{cases}
$$

Appendix B. Simulation parameters

Body

$$
\begin{gathered}
m_1 = 48.0,\ m_2 = 7.0,\ m_3 = 4.0,\ m_4 = 7.0,\ m_5 = 4.0,\\
l_1 = 0.4,\ l_2 = 0.5,\ l_3 = 0.4,\ l_4 = 0.5,\\
I_1 = m_2 l_1^2/3,\ I_2 = m_3 l_2^2/3,\ I_3 = m_4 l_3^2/3,\ I_4 = m_5 l_4^2/3,\\
k_g = 30000.0,\ k_r = 2000.0,\ b_g = 3000.0,\ b_r = 200.0,\\
b = 1.0,\ \beta_w = 2.0,\\
p_1 = 12.5,\ p_2 = 13.5,\ p_3 = 2.5,\ p_e = 150.0,\ p_b = 15.0,\\
x_0 = 0.1\pi\,\text{rad},\ g = 9.8\,\text{m/s}^2.
\end{gathered}
$$

Central pattern generator

τ_i $(i = 1, \ldots, 12)$ are given by

$$
\tau_4 = \tau_{10} = 1/60, \quad \tau_i = 1/30 \text{ (else)}.
$$

τ_i' $(i = 1, \ldots, 12)$ are given by

$$
\tau_3' = \tau_9' = 2.0, \quad \tau_4' = \tau_{10}' = 20/3, \quad \tau_i' = 10/3 \text{ (else)}.
$$

$$
\begin{gathered}
w_{12}, w_{21}, w_{78}, w_{87} = -2.0,\\
w_{17}, w_{71}, w_{28}, w_{82} = -1.0,\\
w_{15}, w_{26}, w_{24}, w_{43}, w_{56}, w_{65} = -1.0,\\
w_{7\,12}, w_{8\,12}, w_{8\,10}, w_{10\,9}, w_{11\,12}, w_{12\,11} = -1.0,\\
\text{otherwise} \quad w_{ij} = 0.0,\\
u_0 = 0.3,\ \alpha_w = 1.0,\ a = 0.7,\ b = 0.8.
\end{gathered}
$$

Initial conditions

$$
\begin{gathered}
x_1 = 0.0,\ x_2 = l_1 + l_2,\ x_3, x_4, x_5, x_6 = 0.0,\\
\dot{u}_i = 0.0,\ \dot{u}_i = 0.0.
\end{gathered}
$$

References

[1] K. Ohgane, S.-I. Ei, H. Mahara: Neuron Phase shift adaptive to time delay in locomotor control, *Applied Mathematical Modelling.* **33** (2009) 797–811.

[2] P.H. Hammond: The influence of prior instruction to the subject on an apparently involuntary neuromuscular response, *J. Physiol.* **132** (1956) 17–18.

[3] C.W.Y. Chan, J.G. Melvill, R.E. Kearney, D.G. Watt: The late electromyographic response to limb displacement in man. I. Evidence for supraspinal contribution, *Electroenceph. Clin. Neurophysiol.* **46** (1979) 173–181.

[4] C.W.Y. Chan, J.G. Melvill, R.F.H. Catchlove: The late electromyographic response to limb displacement in man. II. Sensory origin, *Electroenceph. Clin. Neurophysiol.* **46** (1979) 182–188.

[5] Y. Shinoda, T. Yamaguchi, T. Futami: Multiple axon collaterals of single corticospinal axons in the cat spinal cord, *J. Neorophysiol.* **55** (1986) 425–448.

[6] S. Grillner: Neurobiological bases of rhythmic motor acts in vertebrates, *Science.* **228** (1995) 143–149.

[7] B. Calancie, B. Needham-Shropshire, P. Jacobs, K. Willer, G. Zych, B.A. Green: In voluntary stepping after chronic spinal cord injury. Evidence for a central pattern generator for locomotion in man, *Brain.* **117** (1994) 1143–1159.

[8] M.R. Dimitrijevic, Y. Gerasimenko, M.M. Pinter: Evidence for a spinal central pattern generator in humans, *Ann. NY Acad. Sci.* **860** (1998) 360–376.

[9] G. Taga: Emergence of bipedal locomotion through entrainment among the neuro-musculo-skeltal system and environment, *Physica D.* **75** (1994) 190–208.

[10] S.-I. Ei, K. Ohgane: A new treatment for periodic solutions and coupled oscillators, *Kyushu J. Math.* **65** (2011) 197–217.

[11] K. Ohgane, S.-I. Ei, K. Kudo, T. Ohtsuki: Emergence of adaptability to time delay in bipedal locomotion, *Biol. Cybern.* **90 (2)** (2004) 125–132.

[12] G. Caruso, O. Labianca, E. Ferrannini: Effect of ischemia on sensory potentials of normal subjects of different ages, *J. Neurol. Neurosurg. Psychiat.* **36** (1973) 455–466.

[13] N.B. Mankovskij, N.A. Timko: Age-related characteristics of the functional condition of the neoromuscular system, *Z. Aiterforsch.* **27** (1973) 191–200.

[14] R. Fitzhugh: Impulses and physiological states in theoretical models of nerve membrane, *Biophys.* **H 1** (1961) 445–466.

[15] G. Taga, Y. Yamaguchi, H. Shimizu: Self-organized control of bipedal locomotion by neural oscillators in unpredictable environment, *Biol. Cybern.* **65** (1991) 147–159.

[16] S.-I. Ei: A Remark on the Interpretation of Periodic Solutions, *Bulletin of the Japan Society for Industrial and applied Mathematics.* **14(1)** (2004) 35–47.

[17] Y. Kuramoto: *Chemical Oscillations, Waves, and Turbulence*, Springer-Verlag, Berlin, 1984.

Wulin Weng and Shin-Ichiro Ei
Faculty of Mathematics, Kyushu University, 744 Motooka Nishi-ku, Fukuoka 819-0395, Japan
E-mail: b-oh(at)math.kyushu-u.ac.jp
ichiro(at)math.kyushu-u.ac.jp

Kunishige Ohgane
Graduate school of Arts and Sciences, University of Tokyo, 3-8-1 Komaba Mekuro-ku, Tokyo 153-8092, Japan
E-mail: ohganemath(at)yahoo.co.jp